processes

MDPI

Article

A Simplified Hydrodynamic Model and Automatic Kick Control for Subsea Pump-Lift Dual-Gradient Drilling

Zhiyu Lv [1,*], Guorong Wang [2,3], Xian Wei [1], Lin Zhong [2] and Xuegang Zhang [1]

[1] School of Intelligent Manufacturing, Panzhihua University, Panzhihua 617000, China
[2] College of Mechanical Engineering, Southwest Petroleum University, Chengdu 610500, China
[3] National Key Laboratory of Oil and Gas Reservoir Geology and Exploitation, Southwest Petroleum University, Chengdu 610500, China
* Correspondence: lv_318@163.com

Abstract

Although the world is rich in deepwater oil and gas resources, deepwater drilling faces the challenge of a narrow safety density window. Dual-gradient drilling is an effective approach to address this narrow safety density window, and subsea pump-lift dual-gradient drilling is currently one of the most widely used methods. To improve handling capacity and effectiveness under well kick conditions, we established a simplified hydrodynamic model for subsea pump-lift dual-gradient drilling that accounts for the subsea pump's head-flow performance curve. Based on this hydrodynamic model, we proposed automatic control methods based on throttling regulation and variable-speed regulation and conducted simulation analyses. The results indicate that both control methods can safely, efficiently, and automatically handle well kicks; throttle control has shorter response times and higher precision, while variable-speed control regulates bottom hole pressure by adjusting the subsea pump's rotational speed and offers better energy-saving performance. These findings provide new insights into handling well kicks in subsea pump-lift dual-gradient drilling.

Keywords: dual-gradient drilling; hydrodynamic model; control algorithm

1. Introduction

The world is rich in deepwater oil and gas resources, which are primarily distributed in the Gulf of Mexico, the eastern and western coasts of the Atlantic Ocean, East Africa, North Africa, the Black Sea, the southern Caspian Sea, the Bay of Bengal, the northwestern continental shelf of Australia, and the South China Sea [1]. However, deepwater oil and gas extraction is challenging because of a narrow safety density window, low seawater temperatures, and shallow-layer geological hazards [2]. To address the narrow safety density window in deepwater drilling, Howell proposed dual-gradient drilling technology [3]. Based on their operating principles, dual-gradient drilling technologies primarily include subsea pump dual-gradient drilling, dual-density dual-gradient drilling, riserless dual-gradient drilling, and CAML dual-gradient drilling [4–7]. Among these, subsea pump-lift dual-gradient drilling technology is the most mature and widely applied, having been used in over 1000 wells worldwide to date [8].

As shown in Figure 1, subsea pump-lift dual-gradient drilling technology uses drilling fluid with a higher density than conventional drilling fluid. Through the subsea pump-lift mechanism, the pressure gradient in the return line from the seafloor to the surface is reduced to match seawater density, enabling dual-gradient drilling. Compared with conventional drilling, subsea pump-lift dual-gradient drilling regulates the wellbore pressure

Check for updates

Academic Editor: Muftah El-Naas

Received: 24 August 2026
Revised: 14 September 2026
Accepted: 18 September 2026
Published: 21 September 2026

Copyright: © 2026 by the authors. Licensee MDPI, Basel, Switzerland. This article is an open access article distributed under the terms and conditions of the Creative Commons Attribution (CC BY) license.

profile by adjusting the fluid level in the riser, offering the following advantages: ① it reduces the number of casing strings, thereby lowering drilling costs; ② it extends the openhole drilling limits for large-displacement offshore wells [9]; and ③ it mitigates the risk of wellbore instability while effectively preventing environmental issues such as the direct discharge of drilling fluid into the sea [10]. To achieve safe and efficient drilling, it is necessary to establish a hydrodynamic model to study the processes and mechanisms of hydrodynamic parameter changes under various operating conditions during drilling. Over the years, scholars have conducted in-depth research on hydrodynamic models and control methods for subsea pump-lift dual-gradient drilling systems. Jing Zhou et al. [11] utilized feedback control of the subsea pump to develop an automatic control method for managing well kicks in dual-gradient drilling, designed to maintain bottom hole pressure within the desired range and mitigate well kicks entering the reservoir section during dual-gradient drilling. However, this method is specific to CAML dual-gradient drilling, in which drilling fluid from the riser annulus can flow into the wellbore and bottom hole pressure is regulated via the mud level in the riser. Øyvind Breyholtz et al. [12] used model predictive control (MPC) to control bottom hole pressure and the position of the main hook during drillstring movement by simultaneously controlling the flow rates of the main pump and subsea pump, as well as the drillstring velocity. Li Jiwei [13] established a new mathematical model to simulate unsteady flow in a CAML drilling system. This model predicts transient flow, time to equilibrium, and changes in bottom hole pressure during unstable flow conditions. Yinju Pei et al. [14] (Pei et al., 2021) developed an efficient, energy-saving pressure regulation model (EPRM) for subsea pump-lift systems to enhance the conversion between pressure energy and kinetic energy in dual-gradient control for deep-water drilling. Jing Zeng et al. [15] developed an improved non-chute mud recovery (RMR) system that uses a hybrid chute to create a stable, decoupled circulation path, addressing the environmental and economic challenges associated with conventional subsea discharge of drilling mud. Guorong Wang et al. [16] established a simplified hydrodynamic model for dual-layer pipe, dual-gradient drilling; verified the model's accuracy through onshore well experiments; and designed control algorithms based on flow regulation and pressure regulation. While a substantial body of literature exists on subsea pump-lift dual-gradient drilling technology, detailed studies of well-surging conditions are scarce; in particular, hydrodynamic model studies that account for the impact of subsea pump rotational speed on wellbore pressure are lacking.

Numerical models are widely used in drilling engineering and reservoir stimulation [17–19]. However, advanced hydrodynamic models can improve computational accuracy but require more parameters for calibration, thereby increasing model complexity and computational costs [20]. Kaasa et al. [21] developed a simplified hydrodynamic model based on MPD drilling that reduces model complexity while maintaining computational accuracy. Since then, many researchers have developed control algorithms for MPD based on this simplified hydrodynamic model [22–26], with the aim of more accurately controlling bottom hole pressure. Compared to advanced hydrodynamic models, simplified hydrodynamic models have fewer hydrodynamic parameters and lower computational costs, while still ensuring sufficient accuracy. Building upon this simplified hydrodynamic model, this paper develops a hydrodynamic model for double-gradient drilling using a subsea pump without a riser to reduce model complexity and computational costs. Based on this hydrodynamic model, we established two automatic control models tailored to well-surging conditions: a throttle regulation model and a variable-speed regulation model. We simulated and analyzed well-surging conditions to evaluate the automatic control models' ability to handle well surging and their effectiveness.

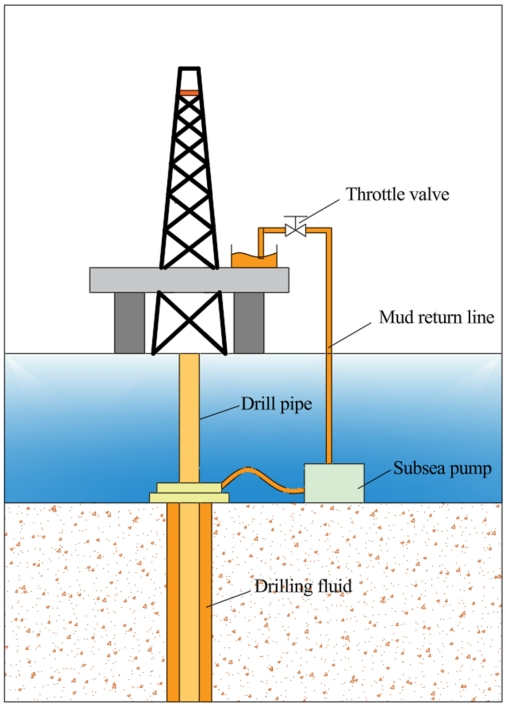


Figure 1. The working principle of the seabed pump-lift dual-gradient drilling technology.

2. Mathematical Model

2.1. Assumptions

To reduce the computational load and ensure the accuracy of the model, the following assumptions are made regarding the hydrodynamic model in this paper:

(1) The effect of phase changes on wellbore pressure is not considered;
(2) The effect of wellbore temperature and pressure on drilling fluid density is not considered;
(3) The effect of drilling fluid viscosity and density on the lift head of the subsea pump is not considered.

2.2. Modeling

Subsea pump-lift dual-gradient drilling is a dual-gradient drilling technique. Its primary operating principle uses a subsea pump to lift the return fluid, reducing pressure in the seawater section and ensuring the pressure gradient in that section matches the density of seawater, enabling dual-gradient drilling. The pumps used in subsea pump-lift dual-gradient drilling are primarily centrifugal; by adjusting the centrifugal pump's rotation speed, the flow rate and head are modified.

Based on the stress–strain equations for the drill pipe and the drilling fluid flow equations [27], a bottom hole hydraulic model for a subsea pump-lift dual-gradient drilling well was developed (as shown in Figure 2).

$$\frac{\partial p}{\partial t} = -\frac{\beta q}{A} \tag{1}$$

$$\frac{\partial q}{\partial t} = -10^9 \frac{A}{\rho_m} \frac{\partial p}{\partial x} - 10^3 \frac{F}{\rho_m} + 1000 A g \cos(\alpha(x)) \tag{2}$$

In the equation, p is pressure, MPa; t is cycle time, s; β is the volumetric modulus of the drilling fluid, MPa; q is the inflow rate, L/s; A is the cross-sectional area of the flow channel, m^2; ρ_m is the density of the drilling fluid, kg/m^3; x is the length of the drilling

fluid column, m; F is the pressure loss per meter of the drilling fluid column, N/m; and g is the local acceleration due to gravity, m/s^2.

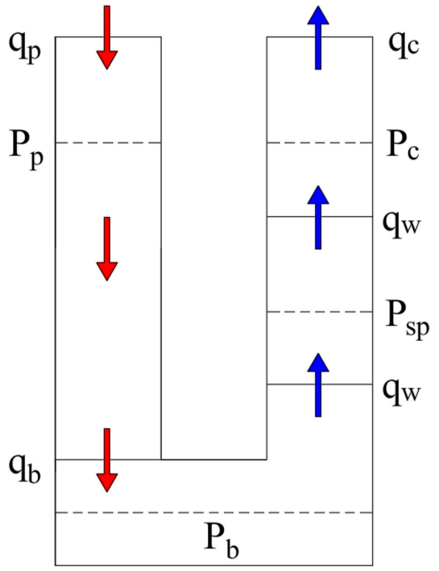


Figure 2. Hydrodynamic model. The red arrows indicate the injection of power fluid, and the blue arrows indicate the return of drilling fluid.

Based on the operating principle of subsea pumps, we established a simplified hydraulic model for subsea pump-lift dual-gradient drilling.

The discharge pressure of the drilling pump is:

$$\dot{p}_{\mathrm{p}} = \frac{\beta_{\mathrm{m}}}{1000 A_{\mathrm{d}} l_{\mathrm{d}}}(q_{\mathrm{p}} - q_{\mathrm{b}}) \tag{3}$$

In the equation, p_{p} is the drilling pump outlet pressure, MPa; β_{m} is the bulk modulus of the drilling fluid, MPa; A_{d} is the cross-sectional area of the drill pipe bore, m^2; l_{d} is the length of the drill pipe, m; q_{p} is the displacement of the drilling pump, L/s; and q_{b} is the discharge rate at the drill bit outlet, L/s.

The flow rate at the drill bit outlet is:

$$\dot{q}_{\mathrm{b}} = 10^9 \frac{A_{\mathrm{d}}}{l_{\mathrm{d}} \rho_{\mathrm{m}}}(p_{\mathrm{p}} - p_{\mathrm{b}}) - 10^9 \frac{F_{\mathrm{d}}(q_{\mathrm{p}}) A_{\mathrm{d}}}{\rho_{\mathrm{m}}} + 1000 A_{\mathrm{d}} g \tag{4}$$

Here, $F_{\mathrm{d}}(q_{\mathrm{p}})$ is the internal pressure loss in the drill pipe, MPa/m.

The friction loss can be calculated using the following formula:

$$F_{\mathrm{d}}(q_{\mathrm{p}}) = 32592.1016 \frac{\rho_{\mathrm{m}}^{0.8} \mu_{\mathrm{m}}^{0.2} {q_{\mathrm{p}}}^{1.8}}{d_{\mathrm{i}}^{4.8}} \tag{5}$$

Here, d_{i} represents the inner diameter of the single-wall drill pipe, mm.

The pressure at the drill bit outlet, i.e., the bottom hole pressure, is:

$$\dot{p}_{\mathrm{b}} = \frac{\beta_{\mathrm{m}}}{A_{\mathrm{a}} l_{\mathrm{a}}}(q_{\mathrm{b}} + q_{\mathrm{kick}} - q_{\mathrm{sp}}) \tag{6}$$

Here, q_{kick} is the well flow rate, L/s; q_{sp} is the flow rate at the subsea pump outlet, L/s.

The change in flow rate at the subsea pump outlet is:

$$\dot{q}_{\mathrm{sp}} = 10^9 \frac{A_{\mathrm{a}}}{l_{\mathrm{a}} \rho_{\mathrm{m}}}(p_{\mathrm{b}} - p_{\mathrm{sp}} + \Delta P) - 10^9 \frac{F_{\mathrm{a}}(q_{\mathrm{b}} + q_{\mathrm{kick}}) A_{\mathrm{a}}}{\rho_{\mathrm{m}}} - 1000 A_{\mathrm{a}} g \tag{7}$$

where A_a is the cross-sectional area of the casing annulus, m^2; l_a is the distance from the well bottom to the subsea pump outlet, m; p_{sp} is the pressure at the subsea pump outlet, MPa; ΔP is the subsea pump boost pressure, MPa; and $F_a(q_b + q_{kick})$ is the pressure loss during lift, MPa/m.

The friction loss can be calculated using the following formula:

$$F_a(q_a + q_{kick}) = 36281.9401 \frac{\rho_m^{0.8} \mu_m^{0.2} (q_a + q_{kick})^{1.8}}{(d_t - d_o)^3 (d_t + d_o)^{1.8}} \tag{8}$$

Here, d_t is the inner diameter of the casing, mm; d_o is the outer diameter of the drill pipe, mm.

The pressure change at the outlet of the subsea pump is:

$$\dot{p}_{sp} = \frac{\beta_m}{1000 A_r l_r} (q_{sp} - q_w) \tag{9}$$

Here, q_w is the wellhead flow rate, L/s.

The change in wellhead flow rate is:

$$\dot{q}_w = 10^9 \frac{A_r}{l_r \rho_m} (p_{sp} - p_c) - 10^9 \frac{F_r(q_{sp}) A_r}{\rho_m} - 1000 A_r g \tag{10}$$

where A_r is the cross-sectional area of the return pipeline, m^2; l_r is the distance from the outlet of the axial-flow pump to the wellhead, m; p_c is the pressure at the throttle valve, MPa; and $F_r(q_{sp})$ is the pressure loss in the return pipeline, MPa/m.

The frictional resistance can be calculated using the following formula:

$$F_r(q_{sp}) = 32592.1016 \frac{\rho_m^{0.8} \mu_m^{0.2} q_{sp}^{1.8}}{d_r^{4.8}} \tag{11}$$

In this case, d_r is the return pipe inner diameter, mm.

The pressure change across the throttle valve is:

$$\dot{P}_c = \frac{\beta_m}{1000 A_p l_p} (q_w - q_c) \tag{12}$$

where q_c is the flow rate through the choke valve, L/s; A_p is the cross-sectional area of the pipeline on the drilling platform, m^2; and l_p is the distance from the wellhead to the choke valve, m.

The flow rate through the choke valve is:

$$q_c = k_c u_c sign(p_c - p_0) \sqrt{|p_c - p_0|} \tag{13}$$

$$q_{kick} = K_{pi}(P_{res} - P_b) \tag{14}$$

In the equation, q_{kick} represents the seepage flow rate, L/s; K_{pi} represents the seepage coefficient, L/(MPa·s); and P_{res} represents the formation pressure, MPa.

Most subsea pumps are vane-type pumps, and their head relates to motor speed and flow rate. When the outer diameter of the vane-type pump impeller is 319 mm, the formula for its head-flow rate characteristic is as follows [28]:

$$n = 103.918(\sqrt{7.242 \times 10^{-7} Q^2 + 6.017H + 1.013 \times 10^{-3} Q^2} - 8.51 \times 10^{-4} Q) \tag{15}$$

In the equation, n represents the rotational speed of the subsea pump, r/min; H represents the head of the subsea pump, m. The performance equation for this subsea pump draws on research conducted by Xia Kailang on subsea pumps; this model was experimentally validated to determine its accuracy [28]. This subsea pump is a DISCP319-125-50-13 vane disk pump [29], with a flow rate of 240 m^3/h, a head of 124 m, an impeller outer diameter of 319 mm, a driven wheel inner diameter of 128 mm, and a disk spacing of 50 mm. This paper primarily establishes a simplified hydrodynamic model of a subsea pump for dual-gradient drilling operations; it is not limited to this specific subsea pump model. If other subsea pump models are required, the corresponding performance curve equations can be substituted.

The work done by the subsea pump on the drilling fluid can be expressed using the Bernoulli equation:

$$\frac{1000P_{in}}{\rho_m g} + \frac{v_{in}^2}{2g} + Z_{in} + H = \frac{1000P_{out}}{\rho_m g} + \frac{v_{out}^2}{2g} + Z_{out} \quad (16)$$

In the equation, P_{in} is the inlet pressure of the subsea pump, MPa; v_{in} is the inlet velocity of the subsea pump, m/s; Z_{in} is the elevation of the subsea pump inlet, m; P_{out} is the outlet pressure of the subsea pump, MPa; v_{out} is the outlet velocity of the subsea pump, m/s; and Z_{out} is the elevation of the subsea pump outlet, m.

The pressure difference across the subsea pump equals the difference between the outlet pressure and the inlet pressure:

$$p_{sp} = P_{out} - P_{in} \quad (17)$$

2.3. Model Validation

To verify the accuracy of the model, validation was conducted from two perspectives. First, the theoretical derivation of the model presented in this paper was supported by the previous research literature. Second, experimental validation was performed using hydrodynamic experimental data.

2.3.1. Preliminary Validation

Kaasa et al. [21] first presented the derivation process for a simplified hydrodynamic model and experimentally validated the accuracy of the model's hydrodynamic parameters. Since this paper presents further research based on the simplified hydrodynamic model, the underlying theory of the model presented here is supported by this work. Subsequently, building upon the simplified hydrodynamic model, Nandan [25], sheikhi [20], Nazir [27], and others proposed new prediction models and control algorithms, such as the nonlinear prediction model, the nonlinear prediction generalized minimum variance (NPGMV) control scheme, and backstepping based controller. The introduction of these models provides strong evidence for the accuracy of the simplified hydrodynamic model. However, most of the above studies were based on MPD technology. For dual-gradient drilling technology, Zhou et al. [11] established a simplified hydrodynamic model and a well kick control algorithm for the CAML dual-gradient drilling technology; based on the principles of dual-casing dual-gradient drilling technology, we established a simplified hydrodynamic model and designed control algorithms, proposing both flow-based and pressure-based control algorithms [16]. The aforementioned studies provide supporting evidence for the further derivation of the model presented in this paper for dual-gradient drilling technology. Therefore, the model in this paper draws upon the results of many previous studies as well as our recent research findings, and its theoretical derivation can be fully substantiated.

2.3.2. Experimental Validation

The experimental validation of the model presented in this paper can draw on experiments conducted on the double-layer pipe dual-gradient drilling model [16]. Due to differences in operating principles—the double-casing, double-gradient drilling system uses a down hole lift pump and double-wall drill pipe, whereas the model in this paper employs a subsea pump and a separate drilling fluid return channel—it is necessary to replace the subsea pump in this model with a down hole lift pump and substitute the corresponding hydraulic parameters in the model with experimental parameters. Fortunately, the experiments measured how bottom hole pressure varies with throttle valve opening while the drilling pump flow rate remains constant. The model in this paper can simulate this process by keeping the subsea pump speed constant and adjusting the throttle, thereby aligning with the experimental conditions and verifying the model's accuracy.

In the research on double-layer pipe dual-gradient drilling technology, laboratory experiments, onshore well tests, and offshore experiments were conducted. Among these, the onshore well tests simulated experiments in which the throttle valve opening was adjusted to measure bottom hole pressure. The testing process utilized double-wall drill pipes, and real-time bottom hole pressure was recorded using down hole logging tools.

Figure 3 shows the experimental validation results. The results indicate that, during the adjustment of the throttle valve opening, the maximum error between the model's calculations and the bottom hole pressure test results did not exceed 0.05 MPa. The experiment validated the accuracy of the model.

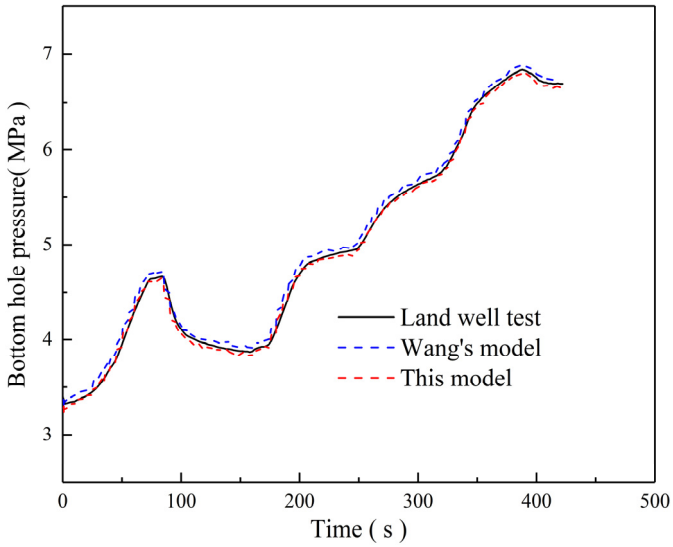


Figure 3. Comparative analysis of simulation results and experimental results.

3. Control Algorithm Design

Based on the subsea pump-lift dual-gradient drilling system and its operating principles, there are two methods of regulation: The first is throttling regulation, which uses the MPD drilling method to control the opening of the throttle valve on the return line, thereby regulating the bottom hole pressure; the second is speed regulation, which, based on the operating principles of subsea pump-lift dual-gradient drilling, adjusts the subsea pump's rotational speed to regulate its flow rate and head, thereby regulating the bottom hole pressure.

(1) Automatic Control Model for Throttling Regulation

Without changing the subsea pump's rotational speed, the bottom hole pressure is regulated by adjusting the opening of the throttle valve on the return line. A PID control method is used to regulate the bottom hole pressure, as follows:

$$n = n_0 \tag{18}$$

$$u_1 = [u_c] \tag{19}$$

$$u_c = K_p e_1(k) + K_i \sum_{i=0}^{k} e_1(i)T + K_d \frac{e_1(k) - e_1(k-1)}{T} \tag{20}$$

$$e_1 = P_{ref} - P_b \tag{21}$$

$$y_1 = [P_b] \tag{22}$$

In the equation, n_0 represents the rotational speed of the subsea pump, r/min; u_1 represents the input parameter of the automatic control model for throttle regulation; u_c represents the throttle valve opening, dimensionless; e_1 represents the bottom hole pressure deviation, MPa; K_p represents the deviation term coefficient, MPa^{-1}; K_i represents the integral term coefficient, MPa^{-1}; K_d represents the derivative term coefficient, MPa^{-1}; P_{ref} represents the formation pressure, MPa; and y_1 represents the output parameter.

(2) Variable-Speed Regulation Automatic Control Model

By adjusting the subsea pump's rotational speed, the pump's head can be adjusted, thereby controlling the bottom hole pressure. Compared with adjusting the throttle valve opening, subsea pump speed regulation is relatively slow and involves power-transmission issues. Therefore, subsea pump speed regulation employs negative feedback control with a set adjustment increment. When a well kick is detected, the subsea pump speed is reduced in fixed increments to increase bottom hole pressure and prevent the well kick from continuing; when bottom hole pressure is detected to be within the safe pressure window, the subsea pump speed remains unchanged; when bottom hole pressure is found to exceed the rupture pressure, indicating drilling fluid loss, the subsea pump speed can be increased. That is:

$$u_c = u_{c0} \tag{23}$$

$$u_2 = [n] \tag{24}$$

$$n_i = \begin{Bmatrix} n_{i-1} + \lambda_n & \text{While } P_b > P_f \\ n_{i-1} & \text{While } P_{res} < P_b < P_f \\ n_{i-1} - \lambda_n & \text{While } P_b < P_{res} \end{Bmatrix} \tag{25}$$

$$y_2 = [P_b] \tag{26}$$

In the equation, u_{c0} represents a specific opening degree of the throttle valve and is dimensionless; u_2 represents an input parameter of the automatic speed control model; n_i represents the current speed of the subsea pump, r/min; n_{i-1} represents the speed of the subsea pump at the previous time step, r/min; λ_n represents the speed control step size of the subsea pump, r/min; P_f represents the formation fracture pressure, MPa; and y_2 represents an output parameter of the automatic speed control model.

4. Results and Discussion

Based on a hydrodynamic model of subsea pump-lift dual-gradient drilling, this study used both a throttling-based automatic control model and a variable-speed regulation automatic control model to simulate hydrodynamic behavior under well kick conditions and evaluate the well kick handling capabilities and performance of the two automatic

control models. In addition, we conducted a case study using the parameters shown in Table 1.

Table 1. Simulation analysis parameters.

Parameters	Values	Units
Q	25	L/s
ρ_m	1200	Kg/m^3
d_i	90	mm
d_o	100	mm
d_t	254	mm
K_{pi}	6.1	L/(s·MPa)

4.1. Throttle Control

PID parameter tuning must be performed before conducting the simulation analysis; the optimization results are shown in Table 2.

Table 2. PID control grid search in the parameter setting process.

Search Parameters	Search Scopes	Search Steps	Optimization Results
K_p	1~8	0.2	3.8
K_i	0~0.06	0.01	0.02
K_d	0~6	0.2	2.6

By adjusting the throttle valve opening on the return line, the throttle valve pressure increases, raising the bottom hole pressure. As shown in Figure 4, after a well blowout occurs, the bottom hole pressure falls below the formation pressure. Within 120 s of the blowout, the blowout is detected, and automatic adjustment begins. At the 120 s mark, the throttle valve opening was adjusted, increasing the throttle valve pressure from approximately 2.92 MPa to 3.4 MPa. At this point, the bottom hole pressure rose from 21.61 MPa to 21.87 MPa, exceeding the formation pressure of 21.8 MPa, and the well kick ceased.

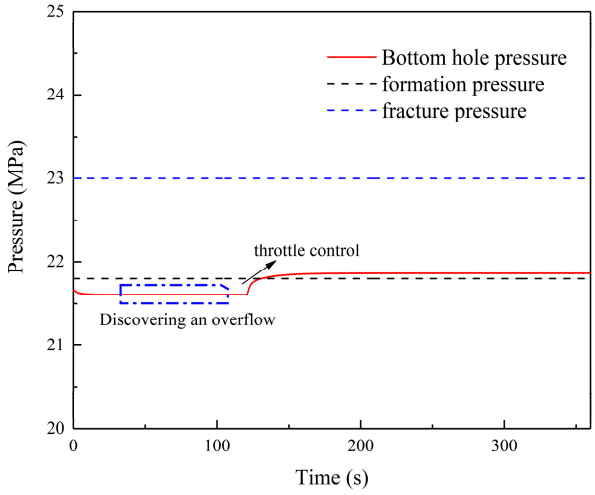


Figure 4. Relationship between bottom-of-well pressure and time under throttle control.

Figure 5 shows the relationship between overflow rate and time under throttle control. As shown in the figure, immediately after the well kick began, the overflow rate increased rapidly to 1.15 L/s, then oscillated around 1.13 L/s. When throttle control was applied

120 s after the overflow began, the well kick flow rate rapidly decreased from 1.15 L/s to 0 L/s. From the start of throttle control at 120 s until the overflow ceased at 131.3 s, a total of 11.3 s elapsed. This relatively short duration indicates that this method can effectively stop overflow in a short period of time.

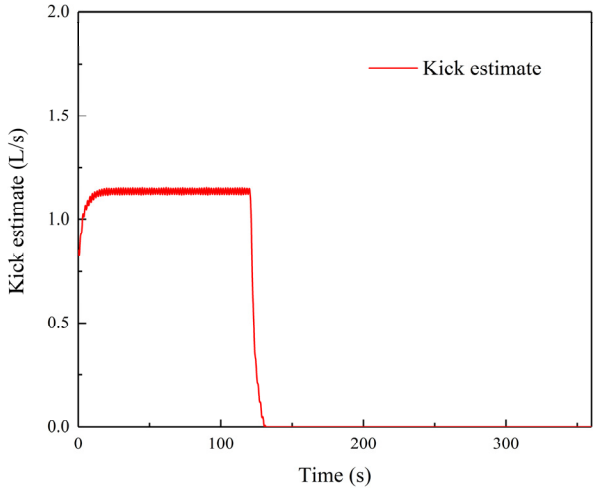


Figure 5. Relationship between overflow flow rate and time under throttle control.

Figure 6 shows the relationship between throttle valve pressure and time under throttle control. As shown in the figure, throttle control was initiated 120 s after the overflow occurred, and the throttle valve pressure increased from approximately 2.92 MPa to 3.4 MPa. However, at 122.8 s, the throttle pressure dropped rapidly from 3.38 MPa to 3.30 MPa, then gradually rose again. Analysis shows that when the throttle valve rapidly closes, the inertia of the drilling fluid exerts a certain impact on the valve, causing sharp fluctuations in pressure near the valve. Because these changes occur very rapidly, the pressure waves do not propagate to the bottom of the well in time; therefore, the bottom hole pressure does not reflect this phenomenon.

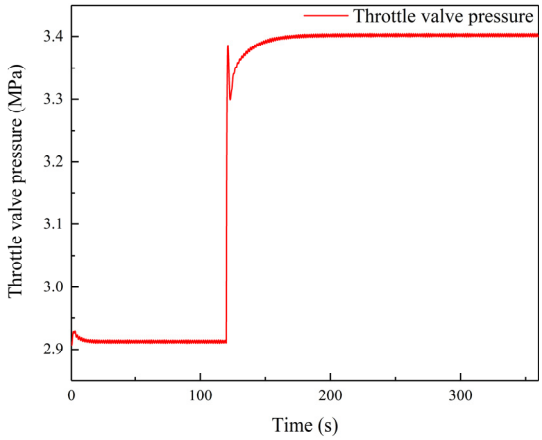


Figure 6. Relationship between throttle valve pressure and time under throttle control.

Figure 7 shows the relationship between the return fluid flow rate and time under throttle control. As shown in the figure, after overflow occurred, the return fluid flow rate reached 26.22 L/s, which was greater than the drilling pump flow rate of 25 L/s. Based on this observable phenomenon, it can be determined that overflow occurred. At 120 s, throttling was used to control the overflow; at this point, the return fluid flow rate decreased from 26.14 L/s to 24.52 L/s, then gradually increased again. The analysis shows that when the valve opening rapidly decreased, some overshoot occurred, causing the

return flow rate to drop to 24.5 L/s. Subsequently, as the overflow ceased, the return flow rate recovered to 25 L/s and fluctuated around that value.

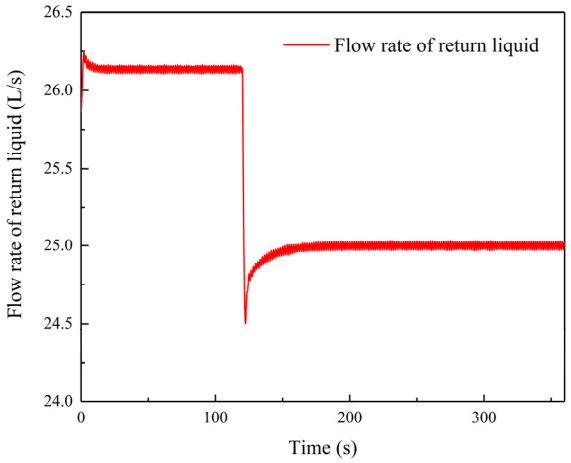


Figure 7. Relationship between return liquid flow rate and time under throttle control.

4.2. Speed-Variable Control

By adjusting the subsea pump speed, the flow rate and head are regulated, thereby controlling bottom hole pressure. After a blowout occurs, reducing the subsea pump's speed decreases its lifting effect on the drilling fluid, thereby increasing the bottom hole pressure and preventing the blowout from continuing. Figure 8 illustrates the relationship between bottom hole pressure and time following a blowout. Similar to the throttle control method, the blowout was detected 120 s after it occurred. Immediately thereafter, speed control was applied to adjust the subsea pump's rotational speed, thereby reducing its flow rate and head and increasing bottom hole pressure. After the blowout, bottom hole pressure stabilized at 21.61 MPa; after 120 s of speed control adjustment, it gradually increased to 21.92 MPa. Compared to throttle control, speed control adjustment took longer and exhibited greater overshoot.

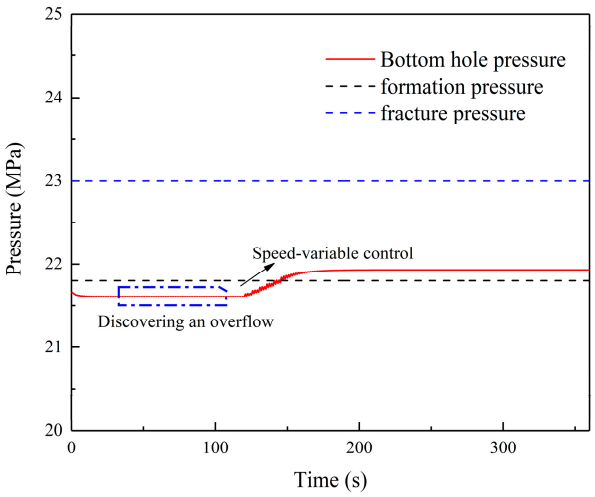


Figure 8. Relationship between bottom hole pressure and time under variable-speed control.

Figure 9 shows the relationship between the overflow rate and time under variable-speed control. As shown in the figure, after overflow began, the overflow rate increased rapidly to 1.15 L/s and then oscillated around that value. Immediately after overflow began, at 120 s, variable-speed regulation was applied to control the overflow rate, which decreased from 1.15 L/s to 0 L/s; however, the overflow rate oscillated across five distinct phases

during this reduction. This was because, during regulation, six consecutive adjustments caused the bottom hole pressure to exceed the formation pressure.

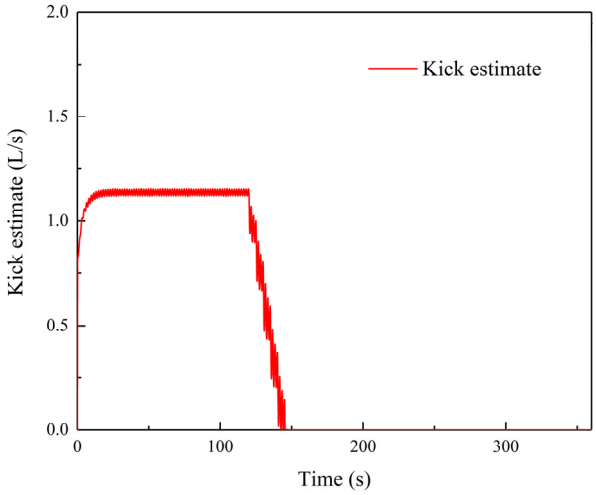


Figure 9. Relationship between overflow flow rate and time under variable-speed control.

Figure 10 shows the relationship between the subsea pump speed and time under variable-speed control. As shown in the figure, the subsea pump speed was adjusted from 2900 r/min to 2780 r/min. We made six adjustments in total, each in equal 20 r/min increments. When the overflow rate equals 0—that is, when the returned fluid flow equals the drilling pump flow—the overflow stops. Since each adjustment was made in fixed increments, some overshoot occurred. As shown in Figure 7, the steady-state bottom hole pressure after the adjustment was 21.92 MPa, representing greater overshoot than the 21.87 MPa steady-state bottom hole pressure achieved through throttle control.

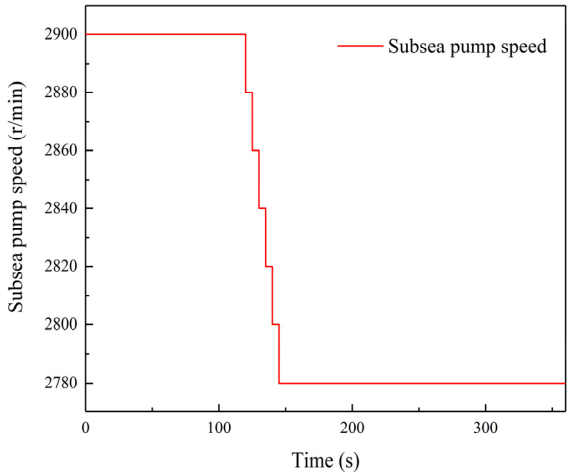


Figure 10. The relationship between the speed of the subsea pump and time under variable-speed control.

Figure 11 shows the relationship between the returned fluid flow rate and time under variable-speed control. As shown in the figure, after an overflow occurred, the returned fluid flow rate increased rapidly, peaking at 26.23 L/s, then fluctuated around 26.14 L/s. At 120 s, the automatic control system detected the overflow and immediately employed variable-speed control to adjust the subsea pump's flow rate and head, thereby increasing the bottom hole pressure. Due to multiple consecutive adjustments to the subsea pump's speed during this process, the return fluid flow rate exhibited significant fluctuations,

dropping to 24.44 L/s. Subsequently, the return fluid flow rate increased to 25 L/s and continued to fluctuate around that value.

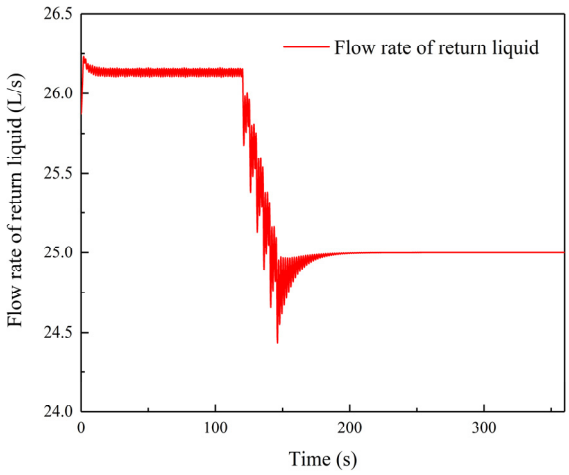


Figure 11. Relationship between return fluid flow rate and time under variable-speed control.

4.3. Comparative Analysis

Figure 12 shows the power consumed by the throttle valve under the two operating conditions. As shown in the figure, before overflow occurs, the power consumed by the throttle valve is the same under both conditions, at 78.2 kW. After overflow occurs, the power consumed by the throttle valve under throttle regulation rapidly increases, reaching approximately 85 kW after overflow control is established; in contrast, after overflow occurs, the power consumed by the throttle valve under speed control mode gradually decreases, reaching approximately 66.6 kW once overflow is controlled. Analysis suggests that throttle control manages overflow by reducing the throttle valve opening, which increases the pressure drop across the valve and consequently raises its power consumption. Speed control regulation manages overflow by reducing the speed of the subsea pump without adjusting the throttle valve opening. Once overflow is controlled, the return fluid flow decreases, reducing the pressure loss across the throttle valve and consequently lowering the power consumed by the throttle valve. This case study demonstrates that speed control regulation is more energy-efficient than throttle regulation, reducing the power consumed by the throttle valve by 18.4 kW.

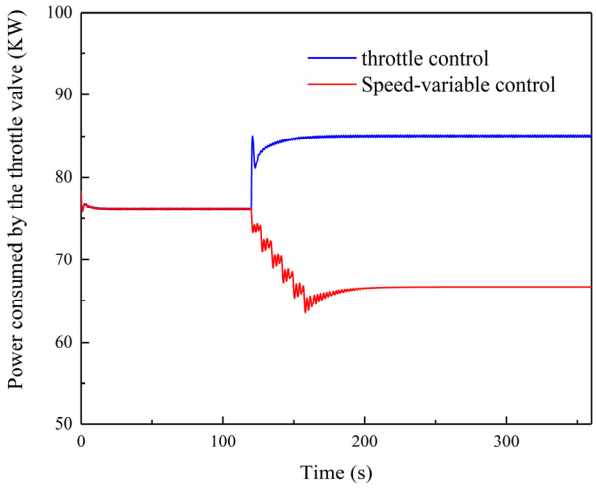


Figure 12. Power consumed by the throttle valve under two operating conditions.

A comparative analysis of throttle control and variable-speed control revealed the following:

(1) Throttle control took less time—11.3 s—while variable-speed control took 25.5 s. The analysis suggests that this is because variable-speed control involves multiple consecutive adjustments to the subsea pump's speed, which also causes significant oscillations during these adjustments.
(2) Speed control exhibits greater overshoot, at 0.12 MPa, whereas throttle control has an overshoot of only 0.07 MPa. This is because speed control adjusts the subsea pump speed in discrete steps, resulting in greater overshoot.
(3) Since variable-speed control reduces the subsea pump's rotational speed, from an energy utilization perspective, variable-speed control is more energy-efficient than throttle control, further reducing drilling costs and conserving resources.

5. Conclusions

Based on the operating principles of subsea pump-lift dual-gradient drilling, the subsea pump head-flow rate performance curve, and formation and wellbore interaction models, this study established a hydraulic model for subsea pump-lift dual-gradient drilling under well kick conditions. Based on this hydraulic model, simulation and analysis of choke control and variable-speed control under well kick conditions were conducted, yielding the following conclusions:

(1) Based on the hydraulic model for subsea pump-lift dual-gradient drilling under well-surging conditions, control models were designed for both throttle control and variable-speed control. Simulation and analysis indicate that both models can automatically handle well-surging conditions.
(2) The throttle control model has a shorter control response time, enabling automatic handling of well-surging conditions within a short period while maintaining high accuracy. However, its energy efficiency is poor; in the case study, the addition of the throttle valve to control well kick increased power consumption by 6.8 kW.
(3) The speed-variation control model has a longer control response time and exhibits some overshoot. Analysis suggests this is due to the need for multiple consecutive adjustments to the subsea pump speed during control; furthermore, the step size used to adjust the speed significantly affects both control response time and accuracy.
(4) Simulations have shown that speed control regulation is more energy-efficient than throttle regulation, reducing the power consumed by the throttle valve by 18.4 kW. From an energy-saving perspective, controlling subsea pump speed improves energy efficiency and supports energy conservation and environmental protection.

Author Contributions: Methodology, Z.L. and G.W.; software, Z.L.; validation, Z.L. and L.Z.; writing—original draft preparation, Z.L. and X.W.; writing—review and editing, Z.L., X.W. and X.Z. All authors have read and agreed to the published version of the manuscript.

Funding: This research was funded by the Panzhihua University Gongga Plan Project, grant number [PUPY11, PUGG09] and the National Natural Science Foundation of China, grant number 52374011.

Data Availability Statement: The data that support the findings of this study are available from the corresponding author upon reasonable request.

Conflicts of Interest: The authors declare no conflicts of interest.

Abbreviations

The following abbreviations are used in this manuscript:

CAML	Controlled Annular Mud Level
RMR	Riserless Mud Recovery
MPD	Managed Pressure Drilling

References

1. Wen, Z.; Wang, J.; Wang, Z.; He, Z.; Song, C.; Liu, X.; Zhang, N.; Ji, T. Analysis of the World Deepwater Oil and Gas Exploration Situation. *Pet. Explor. Dev.* **2023**, *50*, 1060–1076. [CrossRef]
2. Zhang, Z.; Yang, Y.; Qu, Q.; Li, Y.; Zhao, Y.; Xu, Z.; Qiao, Z.; Wang, G.; Zhong, L. Innovations and Challenges in Deepwater Dual-Gradient Drilling: A Review of Current Technologies and Future Directions. *Geoenergy Sci. Eng.* **2025**, *250*, 213829. [CrossRef]
3. Howell, J.D.; Beck, R.W.; Bruce, G.H.; Mclain, J.D. Drilling Fluid Diverter System. U.S. Patent 4063602 A, 20 December 1977.
4. Chen, Q.; Deng, Q.; Tan, L.; Qi, G.; Zhang, J. Status and Prospects of Dual-Gradient Drilling Technologies in Deep-Water Wells. *Front. Energy Res.* **2022**, *10*, 920178. [CrossRef]
5. Stave, R.; Fossli, B.; Endresen, C.; Rezk, R.H.; Tingvoll, G.I.; Thorkildsen, M. Exploration Drilling with Riserless Dual Gradient Technology in Arctic Waters. In *Proceedings of the OTC Arctic Technology Conference, Houston, TX, USA, 10 February 2014*; OTC: Houston, TX, USA, 2014; p. OTC-24588-MS.
6. Stave, R. Implementation of Dual Gradient Drilling. In *Proceedings of the Offshore Technology Conference, Houston, TX, USA, 5 May 2014*; OTC: Houston, TX, USA, 2014; p. D011S002R002.
7. Dowell, J.D. Deploying the World's First Commercial Dual Gradient Drilling System. In *Proceedings of the SPE Deepwater Drilling and Completions Conference, Galveston, TX, USA, 5 October 2010*; SPE: Galveston, TX, USA, 2010; p. SPE-137319-MS.
8. Qin, R.; Lu, Q.; He, G.; Xu, B.; Chen, H.; Li, C.; Yin, G.; Wang, J.; Wang, L. Quantitative Analysis of the Stability of a Mud-Return Circulation System in a Riserless Mud-Recovery Drilling System. *Appl. Sci.* **2023**, *13*, 9320. [CrossRef]
9. Li, X.; Gao, D.; Zhou, Y.; Zhang, H. A Model for Extended-Reach Limit Analysis in Offshore Horizontal Drilling Based on Formation Fracture Pressure. *J. Pet. Sci. Eng.* **2016**, *146*, 400–408. [CrossRef]
10. Yin, Z.; Li, Z.; Huang, X. Scheme Optimization of Deepwater Dual Gradient Drilling Based on the Fuzzy Comprehensive Evaluation Method. *Ocean Eng.* **2023**, *281*, 114978. [CrossRef]
11. Zhou, J.; Nygaard, G. Automatic Model-Based Control Scheme for Stabilizing Pressure during Dual-Gradient Drilling. *J. Process Control* **2011**, *21*, 1138–1147. [CrossRef]
12. Breyholtz, Ø.; Nygaard, G.; Nikolaou, M. Managed-Pressure Drilling: Using Model Predictive Control To Improve Pressure Control During Dual-Gradient Drilling. *SPE Drill. Complet.* **2011**, *26*, 182–197. [CrossRef]
13. Li, J.; Liu, G.; Li, J. Mathematical Modeling of Unsteady Flow in Controlled Mud-Cap Drilling. *Chem. Technol. Fuels Oils* **2016**, *52*, 111–118. [CrossRef]
14. Pei, Y.; Liu, Q.; Wang, C.; Wang, G. Energy-Efficient Pressure Regulation Model and Experiment of Lift Pump System in Deepwater Dual-Gradient Drilling. *Journal of Petroleum Science and Engineering* **2021**, *203*, 108621. [CrossRef]
15. Zeng, J.; Xie, W.; Yu, Y.; Zhang, K.; Chen, H.; Li, B.; Huang, F.; Shen, K.; Lu, Q.; Yu, H. Adaptability Evaluation of Hybrid Riser-Based Riserless Mud Recovery System for Deepwater Natural Gas Hydrate Exploration and Development. *Processes* **2025**, *13*, 1749. [CrossRef]
16. Wang, G.; Lv, Z.; Zhong, L.; Li, Z.; Fu, Q.; Li, Y.; He, Y.; Liu, H. Hydraulic Modeling Study and Control Algorithm Design of Double-Layer Pipe Dual-Gradient Drilling. *Geoenergy Sci. Eng.* **2024**, *240*, 212926. [CrossRef]
17. Ao, F.; Qingchao, L.; Qiang, L.; Jingjuan, W.; Fuling, W.; Chuanliang, Y. Numerical Simulation Investigation of Fracture Propagation Behavior Patterns and Sensitivity Factors of Oil Shale Reservoirs in the Xunyi Region Considering the Influence of Natural Fracture. *Geofluids* **2025**, *2025*, 2762142. [CrossRef]
18. Li, Q.; Wang, F.; Wu, J.; Li, Q.; Zhang, G. Multivariate Coupling Model and Reservoir Characteristics of Enhanced Geothermal Reservoirs. *Energies* **2026**, *19*, 3180. [CrossRef]
19. Wu, J.; Li, Q.; Li, Q.; Wang, F.; Cheng, Y.; Yan, C. Design and Optimization of Bottom-Hole Temperature–Pressure Combinations in Gas Production from Gas Hydrates via Carbon Dioxide Replacement Strategy. *Energies* **2026**, *19*, 3536. [CrossRef]
20. Sheikhi, M.A.; Nikoofard, A.; Khaki-Sedigh, A. Control of Managed Pressure Drilling Systems Using Nonlinear Predictive Generalized Minimum Variance Approach Based on a Volterra Model. *ISA Trans.* **2022**, *128*, 380–390. [CrossRef]
21. Kaasa, G.-O.; Stamnes, Ø.N.; Aamo, O.M.; Imsland, L.S. Simplified Hydraulics Model Used for Intelligent Estimation of Downhole Pressure for a Managed-Pressure-Drilling Control System. *SPE Drill. Complet.* **2012**, *27*, 127–138. [CrossRef]

22. Hauge, E.; Aamo, O.M.; Godhavn, J.-M.; Nygaard, G. A Novel Model-Based Scheme for Kick and Loss Mitigation during Drilling. *J. Process Control* **2013**, *23*, 463–472. [CrossRef]
23. Stamnes, O.N.; Kaasa, G.-O.; Aamo, O.M. Adaptive Estimation of Downhole Pressure for Managed Pressure Drilling Operations. In *Proceedings of the 2011 IEEE International Symposium on Intelligent Control, Denver, CO, USA, 28–30 September 2011*; IEEE: Denver, CO, USA, 2011; pp. 989–995.
24. Zhou, J.; Gravdal, J.E.; Strand, P.; Hovland, S. Automated Kick Control Procedure for an Influx in Managed Pressure Drilling Operations. *Model. Identif. Control Nor. Res. Bull.* **2016**, *37*, 31–40. [CrossRef]
25. Nandan, A.; Imtiaz, S. Nonlinear Model Predictive Control of Managed Pressure Drilling. *ISA Trans.* **2017**, *69*, 307–314. [CrossRef]
26. Li, Q.; Kamel, M. Robustness Analysis and Tuning for Pressure Control in Managed Pressure Drilling. *IFAC-PapersOnLine* **2016**, *49*, 556–561. [CrossRef]
27. Nazir, S.; Ashraf, N.; Ahmad, I. Backstepping Based Control of Heave-Induced Pressure Deviations in Managed Pressure Drilling. In *Proceedings of the 2016 UKACC 11th International Conference on Control (CONTROL), Belfast, UK, 31 August 2016*; IEEE: Belfast, UK, 2016; pp. 1–6.
28. Xia, K. Study on Speed Control and Pressure Management of Subsea Pump for Riserless Hydrate Drilling. Master's Thesis, China University of Petroleum (East China), Dongying, China, 2021.
29. Zhou, C. Research on the Blade Disk Pump for Subsea Mudlift Drilling. Ph.D. Thesis, China University of Petroleum (East China), Dongying, China, 2012.

Disclaimer/Publisher's Note: The statements, opinions and data contained in all publications are solely those of the individual author(s) and contributor(s) and not of MDPI and/or the editor(s). MDPI and/or the editor(s) disclaim responsibility for any injury to people or property resulting from any ideas, methods, instructions or products referred to in the content.